Determination of the Oxide Layer Thickness in Core−Shell Zerovalent Iron Nanoparticles

John E. Martin,[†] Andrew A. Herzing,[‡] Weile Yan,[§] Xiao-qin Li,[§] Bruce E. Koel,[†] Christopher J. Kiely,[‡] and Wei-xian Zhang*,[§]

Center for Advanced Materials and Nanotechnology, Departments of Chemistry, Materials Science and Engineering, and Civil and Environmental Engineering, Lehigh University, Bethlehem, Pennsylvania 18015

Zerovalent iron (nZVI) nanoparticles have long been used in the electronic and chemical industries due to their magnetic and catalytic properties. Increasingly, applications of nZVI have also been reported in environmental engineering because of their ability to degrade a wide variety of toxic pollutants in soil and water. It is generally assumed that nZVI has a core−shell morphology with zerovalent iron as the core and iron oxide/hydroxide in the shell. This study presents a detailed characterization of the nZVI shell thickness using three independent methods. High-resolution transmission electron microscopy analysis provides direct evidence of the core−shell structure and indicates that the shell thickness of fresh nZVI was predominantly in the range of 2−4 nm. The shell thickness was also determined from high-resolution X-ray photoelectron spectroscopy (HR-XPS) analysis through comparison of the relative integrated intensities of metallic and oxidized iron with a geometric correction applied to account for the curved overlayer. The XPS analysis yielded an average shell thickness in the range of 2.3−2.8 nm. Finally, complete oxidation reaction of the nZVI particles by Cu(II) was used as an indication of the zerovalent iron content of the particles, and these observations further correlate the chemical reactivity of the particles and their shell thicknesses. The three methods yielded remarkably similar results, providing a reliable determination of the shell thickness, which fills an essential gap in our knowledge about the nZVI structure. The methods presented in this work can also be applied to the study of the aging process of nZVI and may also prove useful for the measurement and characterization of other metallic nanoparticles.

Introduction

Very fine particles of metallic or zerovalent iron have been studied for many years. Since iron is one of the most useful magnetic materials, it has been widely used as a magnetic recording medium. Nanosized magnetic iron is the key material behind the recent development of rewritable electronic media. Improvements in the production of nanosized iron have led to rapidly growing capacities and shrinking component sizes in many electronic products. Other notable applications of nanoscale iron include use in the diagnosis and treatment of medical diseases and as electronic sensors and transformers. Furthermore, iron is also a classic catalyst used in the formation and cleavage of carbon−carbon bonds (e.g., the Fischer−Tropsch synthesis).[1,2]

Nanoscale zerovalent iron (nZVI) is also an effective reagent for treatment of toxic and hazardous chemicals. As a strong reductant, nZVI can degrade a wide range of pollutants by adsorption and chemical reduction.[3,4] Both organic (e.g., chlorinated hydrocarbons) and inorganic (nitrate, chromate, perchlorate, metal ions) pollutants in the environment can be treated with nZVI.[3−9] Favorable chemical and structural factors

contribute to the increasing environmental applications of nZVI. Chemically, zerovalent iron serves as a cost-effective and environmentally friendly reductant.[2,3] Structurally, the small size of nanoparticles provides a high surface-to-volume ratio, which promotes mass transfer to and from the solid surface and increases the adsorption and reaction capacity for contaminant removal and degradation. In engineering practice, the small size offers the combined advantage of easy mixing and potential mobility in groundwater.[2,3]

It is generally accepted that nZVI has a core−shell structure with a zerovalent iron core surrounded by an iron oxide/hydroxide shell, which grows thicker with the progress of iron oxidation.[5−7] However, it is difficult to measure the exact thickness of the shell due to the high reactivity of iron, which reacts very rapidly with both oxygen and water and may even oxidize in air. Traditionally, the shell thickness is estimated on the basis of measurement of the zerovalent iron content, which is determined from its corrosion rate and/or production of hydrogen gas. However, such experiments are tedious, are time-consuming and often use hazardous chemicals.

Detailed structural characterization is essential to understand how the structure of nZVI relates to its activity. The nZVI structure depends on how the nanoparticles are synthesized,[2,10] and in this work we focus on fresh nZVI produced chemically by the

* To whom correspondence should be addressed. E-mail: wez3@lehigh.edu.
† Department of Chemistry.
‡ Department of Materials Science and Engineering.
§ Department of Civil and Environmental Engineering.

(1) Huber, D. L. *Small* **2005**, *5*, 482−501.
(2) Li, X.; Elliott, D.; Zhang, W. *Crit. Rev. Solid State Mater. Sci.* **2006**, *31*, 111−122.
(3) Masciangioli, T.; Zhang, W. X. *Environ. Sci. Technol.* **2003**, *37*, 102A-108A.
(4) Zhang, W. *J. Nanopart. Res.* **2003**, *5*, 323−332.
(5) Li, X.; Zhang, W. *J. Phys. Chem. C* **2007**, *111*, 6939−6946.
(6) Li, X.; Zhang, W. *Langmuir* **2006**, *22*, 4638−4642.
(7) Nurmi, J. T.; Tratnyek, P. G.; Sarathy, V.; Baer D. R.; Amonette, J. E.; Peacher, K. et al. *Environ. Sci. Technol.* **2005**, *39*, 1221−1230.
(8) Ponder, S. M.; Darab, J. G.; Mallouk, T. E. *Environ. Sci. Technol.* **2000**, *34*, 2564−2569.
(9) Hydutsky, B. W.; Mack, E. J.; Beckerman, B. B.; Skluzacek, J. M.; Mallouk, T. E. *Environ. Sci. Technol.* **2007**, *41* (18), 6418−6424.
(10) Sun, Y.; Li, X.; Cao, J.; Zhang, W.; Wang, H. *Adv. Colloid Interface Sci.* **2006**, *120*, 47−56.

reduction of iron salts. This method was previously shown by X-ray photoelectron spectroscopy (XPS) to produce core−shell particles.[5,10] These particles were also analyzed by transmission electron microscopy (TEM) and light scattering methods[7,10] and found to be polydisperse with an average diameter of approximately 60 nm and a standard deviation of 15 nm.[10] TEM analysis also indicated that the shell thickness varied significantly; however, a full statistical determination of the thickness has not yet been carried out.

XPS is a powerful tool for probing the surface and near-surface composition and chemical state (oxidation state). As depth increases, photoelectrons ejected from the surface layer or near-surface region (up to 10 nm or so typically) of a sample being analyzed decrease and can be precisely detected in XPS. Quantitatively, a sampling depth can be defined on the basis of the inelastic mean free path for electron scattering or the attenuation length, λ, which is the thickness of material through which electrons may pass with a probability e^{-1} that they survive without inelastic scattering and thus are detected at their characteristic energies.[11] Knowledge of these attenuation lengths can be used with XPS data to provide information on the concentration variations with depth in the near-surface region for nonhomogeneous distributions within the sample. Analysis often requires a model to be assumed for this distribution, but it is common to analyze flat, planar films and layers by comparing the relative intensity of signals characteristic of the bulk and film or overlayer.[12] Effects such as surface roughness can also be accounted for by geometrical corrections.[13−15]

In this study, the thickness of the nZVI oxide shell was determined by three independent methods: (i) high-resolution TEM imaging, (ii) high-resolution XPS, and (iii) chemical oxidation of ZVI. TEM analysis provides direct images of the core−shell structure and the dimension and variation of the shell thickness in the area analyzed. However, even though the TEM technique has very good spatial resolution, it inherently has rather poor sampling statistics. HR-XPS analysis, by comparing the intensities of metallic versus oxidized iron core-level peaks, was applied to calculate the mean and standard deviation of the distribution of shell thicknesses by using a geometrical correction to account for the spherical shape of the nanoparticles.[14] This thickness determination was compared with a magic angle analysis where topographical effects are limited.[17] Furthermore, the average shell thickness can be estimated independently on the basis of the sample total mass and metallic iron content of the sample determined by using stoichiometric oxidation of iron with Cu(II).

Experimental Methods

nZVI Synthesis. Nanoscale zerovalent iron particles were prepared as previously reported.[2,3] Briefly, $FeCl_3 \cdot 6H_2O$ (0.05M) was reduced by titration with $NaBH_4$ (0.2 M) in a vigorously stirred reaction flask. The iron nanoparticle precipitate was collected with vacuum filtration and washed with deionized water. The nanoparticles were dried and stored in a nitrogen-purged atmosphere to minimize oxidation prior to analysis.

(11) Seah, M.; Dench, W. *Surf. Interface Anal.* **1979**, 1, 2−11.
(12) Fadley, C. In *Basic Concepts of X-ray Photoelectron Spectroscopy*; Brundle, C., Baker, A., Eds.; Electron Spectroscopy: Theory Techniques and Applications Vol. 2; Academic Press: New York, 1978; p 1.
(13) Gunter, P.; Niemantsverdriet, J. *Appl. Surf. Sci.* **1995**, *89*, 69−76.
(14) Mohai, M.; Bertoli, I. *Surf. Interface Anal.* **2004**, *36*, 805−808.
(15) Gillet, J.; Meunier, M. *J. Phys. Chem. B* **2005**, *109*, 8733−8737.
(16) Varsanyi, G.; Mink, G.; Ree, K.; Mohai, M. *Period. Polytech.* **1986**, *2*, 3−17.
(17) Kappen, P.; Reihs, K.; Seidel, C.; Voetz, M.; Fuchs, H. *Surf. Sci.* **2000**, *465*, 40−50.

TEM Observations. Specimens were prepared for TEM analysis by allowing a drop of nZVI suspension in ethanol to evaporate onto a lacey carbon film supported by a 300-mesh copper TEM grid. The shell thickness and structural morphology of the iron particles were then analyzed using a JEOL 2000FX transmission electron microscope equipped with a LaB_6 filament and operating at 200 kV.

XPS Measurements. HR-XPS was carried out on nZVI material using a Scienta ESCA-300 instrument. Samples were prepared by pressing the nZVI onto a conductive adhesive. High resolution in XPS was achieved by using a combination of a rotating anode X-ray source operated at 3.8 kW and a seven-crystal monochromator to produce 1486 eV Al Kα X-rays and a 300 mm mean radius hemispherical electrostatic analyzer and multichannel plate CCD camera for electron energy analysis. HR-XPS spectra were obtained at several takeoff angles, primarily at 90° and 35° with respect to the sample surface plane. Binding energies (BEs) reported are referenced to the adventitious C 1s peak at 284.6 eV BE.

Estimation of the Oxide Layer Thickness by the Chemical Oxidation of Iron with Copper(II). When metallic iron is in contact with Cu(II) ion in aqueous solution, a galvanic cell is established. At the anode, Fe^0 is oxidized to Fe(II), and the electrons are consumed by the Cu(II) ion at the cathode to form Cu^0 as shown in the following equation:

$$Cu^{2+}(aq) + Fe^0(s) \rightarrow Cu^0(s) + Fe^{2+}(aq) \tag{1}$$
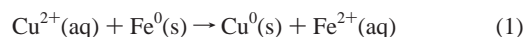
In an oxygen-free solution at near-neutral pH, the reduction of water by nZVI is relatively slow and reaction 1 dominates in the solution.[18] The kinetics of the above reaction have been studied, and the rate scales with the surface area of iron metal.[19,20] In addition, it has been demonstrated that nanoscale iron particles, with a surface area on the order of 20−30 m^2/g, are able to reduce copper ions rapidly.[5] From the quantity of copper reduced, the amount of Fe^0 originally present in the nanoparticles can be estimated, and thereby, the thickness of the oxide layer can be deduced by a simple calculation involving the total mass of the nanoparticle sample.

To carry out this measurement, aqueous Cu(II) solutions were prepared from cupric chloride salt. The solution was purged with nitrogen for 30 min prior to addition of ZVI nanoparticles to strip away any dissolved oxygen from the water. A set of experiments were conducted at various initial concentrations of Cu(II) with the iron nanoparticle concentration fixed at 0.25 g/L. The bottles were capped, tape-sealed, and agitated for 1 h. After the reaction, the solutions were filtered, and the concentrations of Cu(II) remaining in the aqueous phase were analyzed by an atomic absorption spectrometer (Perkin-Elmer AAnalyst200).

Results and Discussion

The surface morphology of nZVI is shown in Figure 1. The fresh nZVI particles are generally spherical in shape with the majority in the size range of 50−100 nm. A close-up image (Figure 1b) reveals that the particles are connected in chains due to magnetic dipole interactions and chemical aggregation. A few large flaky materials are oxidized products of nZVI. Results from high-resolution TEM analysis of the nZVI particles are given in Figure 2, which shows both selected-area electron diffraction data and representative bright-field TEM micrographs. Analysis of electron diffraction ring patterns (Figure 2a) obtained from the nZVI sample confirmed that the nZVI particles consisted of very fine crystallites of bcc Fe as evidenced by the presence of diffuse characteristic {110}- and {200}-type rings. Bright-field TEM imaging (Figure 2b,c) showed that the agglomerates of nanocrystalline Fe particles (typically 50−150 nm in size) were always surrounded by a thin shell of amorphous material, which we have previously assigned as FeOOH.[6,10] The coating,

(18) Speller, F. N. *Corrosion, Causes and Prevention*, 3rd ed.; McGraw-Hill: New York, 1951.
(19) Khudenko, B. M.; Gould, J. P. *Water Sci. Technol.* **1991**, *24*, 235−246.
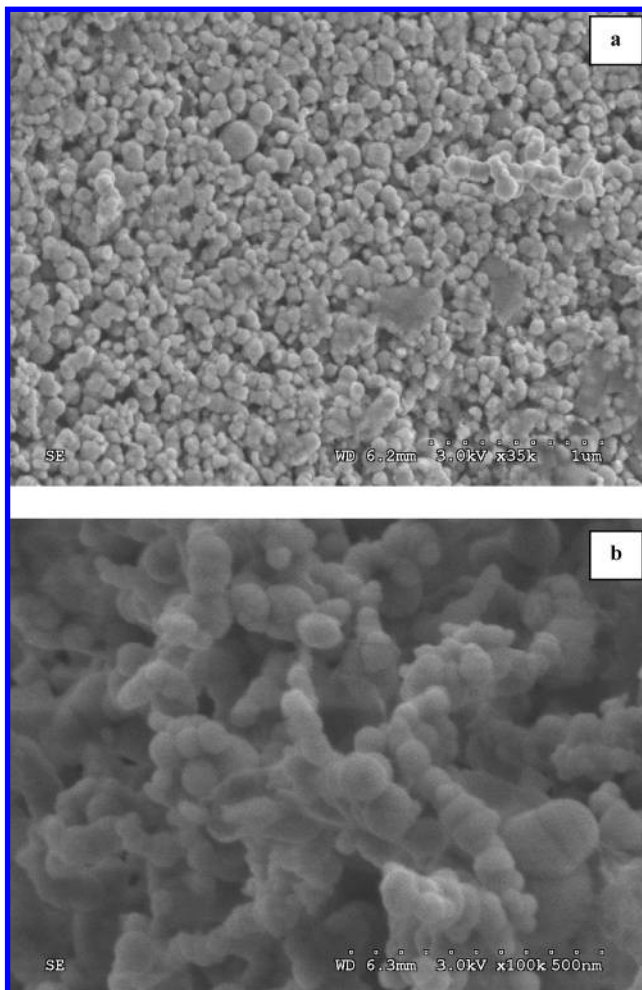(20) Miller, J. D.; Beckstead, L. W. *Met. Trans.* **1973**, *4*, 1967−1973.

Figure 1. SEM images of nZVI particles.

i.e., shell, thickness was found to vary significantly, not only between different nZVI particles, but also around each individual particle. Predominantly, the FeOOH layers were in the range of 2−4 nm in thickness (Figure 2b), although shells as thick as 25 nm and as thin as 1 nm were occasionally observed in isolated regions (Figure 2c).

Using XPS, a survey scan from 0 to 1100 eV BE was acquired for the as-prepared nZVI sample, as shown in Figure 3. This broad, low-resolution scan indicates the predominate elements present in the near-surface region of the sample. Figure 3 shows the presence of principally iron and oxygen, as indicated by the Fe $2p_{3/2}$ peaks at 715 eV BE and the O 1s peak at 530 eV BE. In addition, adventitious carbon on the sample is indicated by a peak at 284.6 eV BE, and peaks at 1071 and 182 eV BE from Na 1s and B 1s, respectively, indicate considerable concentrations of Na and B from residual $NaBH_4$ from the synthesis.

Iron detected in this survey scan can be attributed to metallic iron within the core of the particles as well as iron oxides and iron oxyhydroxide, FeOOH, within the shell.[5,6,10] This differentiation of the iron chemical (oxidation) states can be performed by taking a high-resolution scan of the Fe 2p region in XPS. Because the Fe $2p_{1/2}$ and $2p_{3/2}$ spin−orbit split peaks in XPS reveal the same chemical information, we show only the more intense Fe $2p_{3/2}$ region in Figure 4. As expected, we observed chemically shifted peaks due to metallic iron, Fe^0, and from oxidized iron, Fe^{3+}. Figure 4 establishes clearly that some metallic iron remains in the nZVI, in the core of the particles; however, it is not obvious by inspection how much metallic iron is present and, in particular, the thickness of the oxidized iron shell. XPS
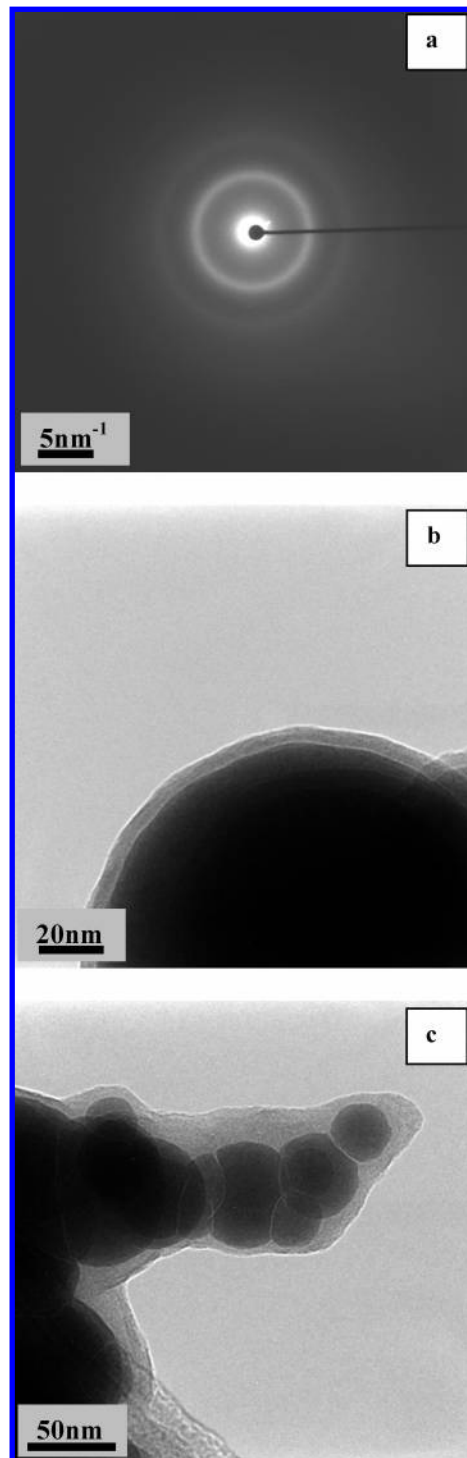

Figure 2. TEM analysis of nZVI particles: (a) selected-area electron diffraction ring pattern confirming that the particles consist of very fine bcc Fe crystallites; (b, c) representative bright-field TEM micrographs of nZVI particles illustrating that all particles are covered by a thin coating or shell and that the majority of the shells observed are 2−4 nm in thickness, but this could vary from 1 to 25 nm in some areas.

is a quantitative analytical technique, and the intensity of the Fe 2p signal in XPS is proportional to the number of Fe atoms in the sampled near-surface region. This relationship is independent of the Fe atom environment, i.e., independent of the Fe oxidation state, so in principle the relative amount of oxidized iron and metallic iron in the sample can be calculated by analysis of a spectrum such as that shown in Figure 4. In this analysis, a
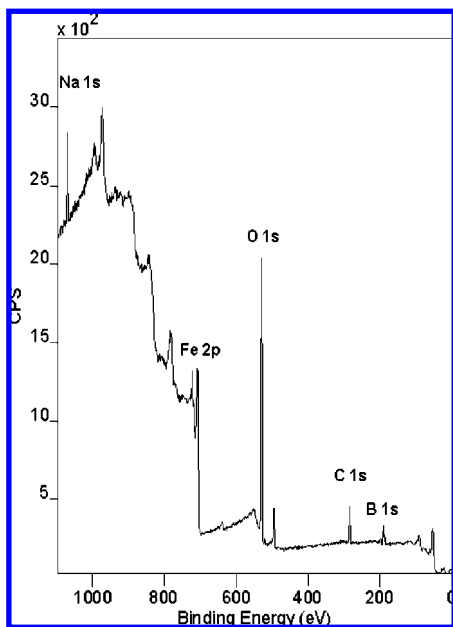
Figure 3. Broad survey scan in XPS of the nZVI sample.

Figure 4. High-resolution XPS scan of the Fe $2p_{3/2}$ region for the nZVI sample.

Shirley-type background subtraction was applied to distinguish the Fe 2p photoelectron peaks from an inelastic scattering background. The $2p_{1/2}$ and $2p_{3/2}$ peaks for both Fe^{3+} and Fe^0 were assigned individual Gaussian−Lorentzian components for deconvolution, and the area under each peak was integrated. A relative intensity ratio, 0.233, was determined as the sum of the $2p_{1/2}$ and $2p_{3/2}$ areas for Fe^0 divided by the corresponding areas of the $2p_{1/2}$ and $2p_{3/2}$ signals for Fe^{3+}.

The nZVI shell thickness was calculated with XPS Multiquant software using a geometric correction to compensate for spherical topography.[14,21,22] For a metal covered by a metal oxide layer with a flat topography, the relative intensity of zerovalent to oxidized metal is defined by[22]

$$\frac{I_{me}}{I_{ox}} = \frac{N_{me}\lambda_{me}}{N_{ox}\lambda_{ox}} \frac{\exp[-d/(\lambda_{ox}\cos\theta)]}{1 - \exp[-d/(\lambda_{ox}\cos\theta)]} \qquad (2)$$

where I_{me} is the photoelectron intensity of the metal, I_{ox} is the intensity of the oxidized metal, N is the number of atoms per unit volume, λ is the inelastic mean free path, d is the oxide layer thickness, and θ is the detection angle. Thus, the layer thickness can be calculated as[22]

$$d = \lambda_{ox}\cos\theta\,\ln\!\left(\frac{N_{me}\lambda_{me}}{N_{ox}\lambda_{ox}}\frac{I_{ox}}{I_{me}} + 1\right) \qquad (3)$$

However, for a core−shell nanoparticle, the curved surface of the nanoparticle causes changes in the relative intensity of photoelectrons originating from the core or shell. For a detector placed above the sample surface, photoelectrons escaping from the edge of a nanoparticle will originate predominantly from the shell while those photoelectrons escaping from the apex will more likely emanate from both the core and shell. Although the shell thickness may be constant around the particle, the effective thickness, d^{eff}, will vary at different positions across the diameter of the nanoparticle, as shown in Figure 5.[14] These values are determined by dividing the top hemisphere of the particle into slices at different angles. The intensity is calculated at each position and is weighted by a geometric correction factor which
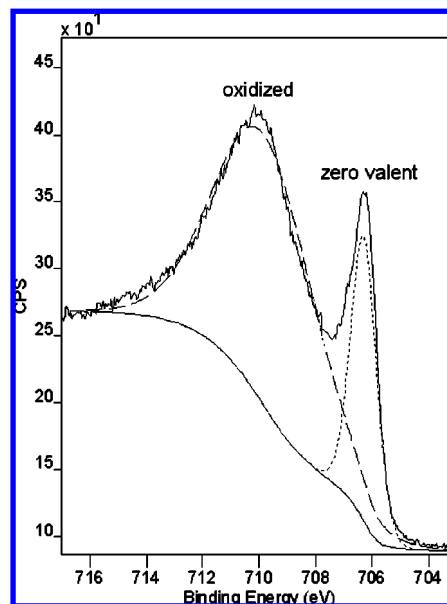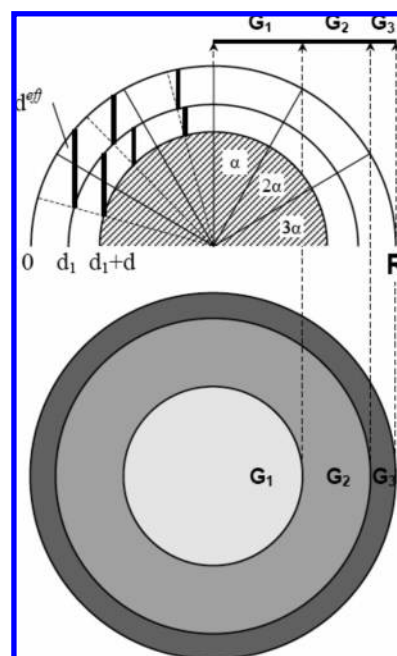

Figure 5. Schematic drawing showing the axial cross-section of a core−shell nanoparticle in which the particle has been divided into several zones for calculating intensities in XPS.

depends on the zone (G1, G2, etc.), or angle within the nanoparticle, from which the intensity is measured.[14] The experimental intensity is then corrected as the sum of intensities from the weighted zones. Since the nanoparticles were analyzed in powder form, a second correction was applied to account for signals originating from lower layers of spheres.

The inelastic mean free path was calculated using the CS2 semiempirical method.[23] This is based on calculations of the attenuation length, λ_{AL}, developed by Cumpson and Seah.[23] The CS2 semiempirical method[23] states that

$$\lambda_{AL} = 0.316a^{3/2}\left\{\frac{E}{Z^{0.45}[\ln(E/27) + 3]} + 4\right\} \qquad (4)$$

(21) Mohai, M. *Surf. Interface Anal.* **2004**, *36*, 828−832.
(22) Mohai, M. *XPS Multiquant Users Manual*; 2005.

Table 1. Thickness Determination for Varying Average Particle Diameters

diameter (nm)	10	20	30	40	50	60	100	200
shell thickness (nm)	2.85	2.57	2.49	2.45	2.42	2.40	2.38	2.36

where a is the lattice parameter or monolayer thickness (nm), E is the kinetic energy, and Z is the average atomic number. Since the relative intensities are from the same element, corrections for sensitivity factors or contamination need not be applied.
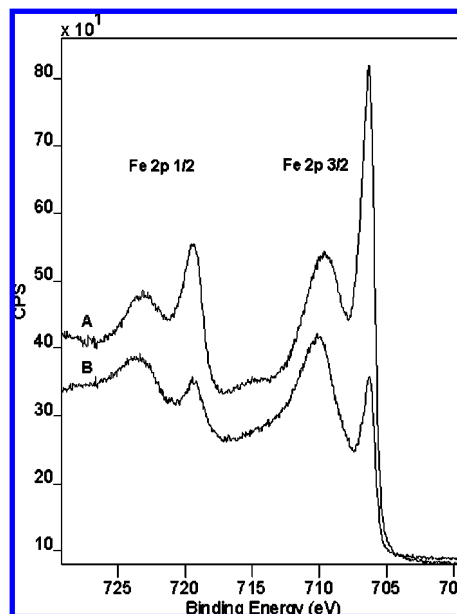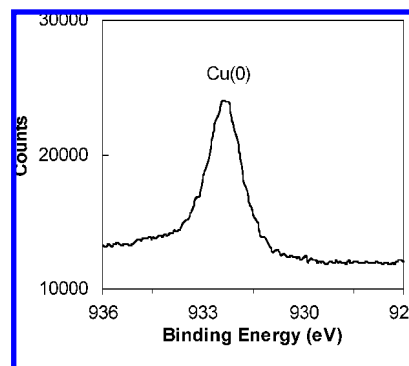
For Fe photoelectrons moving through the metallic core and oxide shell, $\lambda_{me} = 1.10$ nm and $\lambda_{ox} = 1.42$ nm. One limitation of this model is that the thickness can only be determined if the layer is within a certain range. This range is governed by the sampling depth of the photoelectrons analyzed, with a maximum sampling depth of approximately several multiples of λ. Therefore, the XPS technique is most accurate for measurements of oxide layers less than $5-10$ nm in thickness.

The density of bulk iron, 7.87 g/cm^3, and bulk goethite (FeOOH), 4.28 g/cm^3,[24] were utilized to approximate the density of the core and shell layers. It has been shown by TEM and light scattering methods that the median nanoparticle diameter was 60 nm.[10] On the basis of this particle size, the calculated average shell thickness was 2.4 nm.

The effect of varying diameter was assessed because these nanoparticles are very polydisperse, possessing a broad range of sizes. Since the distribution of particle diameters was mainly between 10 and 200 nm,[10] the thickness was calculated at intervals within this range (Table 1). On the basis of these values, the maximum error due to polydispersity was calculated. For a constant intensity, a nanoparticle of 10 nm diameter has a thickness of 2.85 nm and a particle of 200 nm diameter a thickness of 2.36 nm. This provides a maximum error of ± 0.25 nm. On the basis of this model, most of the error is attributed to the smaller nanoparticles. This is because the effects of the edge are slightly more exaggerated for smaller particles. The relatively narrow range of the average shell thickness reflects the nature of the shell formation in that the thickness is controlled by the rate of mass or electron transfer across the oxide layer.

It has been shown that topographical effects on this analysis can be reduced at an off-normal "magic angle".[13,17] Specifically, at 55° off-normal (away from a direction perpendicular to the sample surface), the ratio between the observed thickness, d_{obs}, and the true thickness, d_o, is constant; $d_{obs}/d_o = 1.6$. The relative intensity ratio of the metal signal to the oxide signal measured at 55° was found to be 0.283. Thus, using eq 2, the observed oxide thickness is calculated to be 3.1 nm, giving a true thickness of approximately 1.9 nm. This value agrees reasonably well with the thickness determined via the initial geometric correction (2.4 nm), which was expected to be higher because the edges of nanoparticles contribute to a higher shell signal. While angle-dependent analysis can be applied readily to flat samples because lower angles correlate with higher surface sensitivity, ideally the signal from a nanoparticle should not depend on the angle since the thickness determination is constant at all angles. However, self-shadowing and neighboring particle shadowing effects complicate the analysis, and therefore, a magic-angle analysis can be very useful in overcoming these effects.

To further verify the presence of a core−shell structure in the nZVI particles, a sputtering technique that has been previously illustrated[16] was employed. By sputtering the nanoparticles using

(23) Cumpson, P.; Seah, M. *Surf. Interface Anal.* **1997**, *25*, 430−446.
(24) Yang, H.; Lu, R.; Downs, R.; Costin, G. *Acta Crystallogr., Sect. E: Struct. Rep. Online* **2006**, *E62* (12), i250−i252.

Figure 6. Fe 2p region in XPS for the nZVI sample (A) after and (B) before sputtering.

Figure 7. High-resolution XPS scan of the Cu 2p$_{3/2}$ region showing the presence of a peak at 932.4 eV BE indicative of Cu^0.

10^{-5} Torr of Ar, the top layers were removed and the relative intensity ratio of Fe/Fe^{3+} increased from 0.233 to 0.608 (Figure 6). This correlates well with iron oxides and oxyhydroxides in the shell being sputtered away and the metallic iron core being exposed. Also, the oxidized Fe 2p$_{3/2}$ peak shifts from 710.2 to 709.6 eV BE, and this shift has been attributed to reduction of Fe^{3+} during sputtering.[25] An extensive depth profile was not performed due to the spherical topography. Other XPS analyses can be used to provide the oxide shell thickness on the basis of the sampling depth of photoelectrons. Since XPS is only sensitive to the outer $3-5$ nm of a solid, the presence of an Fe^0 peak suggests the shell was on the order of a few nanometers thick.[7]

Another approach to estimate the shell thickness is to experimentally measure the content of zerovalent iron in the particles, which can be done in a number of ways. For example, some researchers have measured the amount of hydrogen gas produced from iron reactions with water.[7] The speedy reaction of nZVI is exploited for the fast measurement of the zerovalent iron content. We tested the rapid and complete reduction of Cu(II) with nZVI to independently verify the results obtained by both TEM and XPS analysis.

In a laboratory batch study, 0.25 g/L nZVI was added to a solution with 200 mg/L Cu(II). The reaction was fast with more than 80% of the Cu(II) removed from solution in less than 1 min

(25) Mills, P.; Sullivan, J. *J. Phys. D: Appl. Phys.* **1983**, *16*, 723−732.
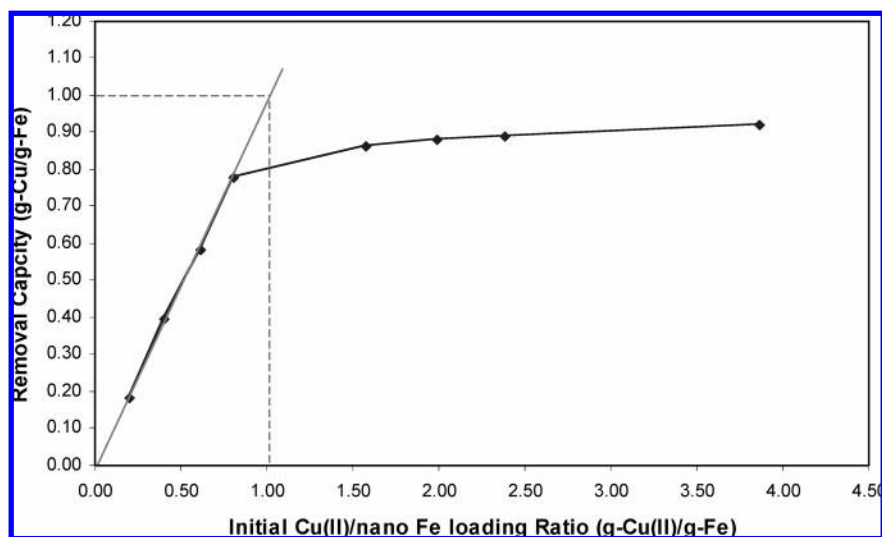
Figure 8. Cu(II) removal capacity of nZVI showing two behavioral domains. The initial concentration of Cu(II) varied from 50 to 1000 mg/L, with the concentration of iron nanoparticles fixed at 0.25 g/L. The auxiliary line shown in gray represents the case where Cu(II) is completely removed by iron.

and near-complete uptake of Cu (>99%) in 2 min. Figure 7 gives the XPS spectrum of the Cu $2p_{3/2}$ region for the nZVI particles after the particles were reacted with copper.[5] A peak at 932.4 eV BE arises from Cu(0), suggesting that Cu(II) was reduced and immobilized on nZVI. To exclude the possibility that the Cu signal is from precipitation of copper hydroxide, the solution pH was measured after reaction and found to be in the range of 4−5, thus ensuring that the Cu was indeed immobilized on the nZVI particles.

Figure 8 shows the removal of iron particles at different Cu(II)-to-Fe ratios. The shape of the curve indicates that two domains of reaction can occur. At low initial Cu(II) concentration, the Cu(II) being removed per gram of iron nanoparticles increases with the initial copper concentration. The match of the experimental data to the auxiliary line, which represents the scenario for complete removal of the Cu(II), indicates all Cu(II) is sequestrated when iron is present in excess. Any further increase in copper concentration causes iron to be limiting, and the curve approaches a plateau. The maximum reduction capacity can thus be estimated.

As shown in Figure 8, the total reduction is approximately 0.922 g of Cu(II)/g of iron nanoparticles. Since 1 mol of Fe^0 is consumed for every mole of Cu^{2+} reduced, the mass fraction of Fe^0 in the nanoparticles is calculated as 0.810 g of Fe^0/g of nanoparticles. Using a median particle diameter of 60 nm and the bulk densities of Fe^0 and FeOOH given earlier, the thickness of the oxide shell is estimated to be 3.4 nm. This is in very good agreement with the TEM and XPS results considering that the calculation of the shell thickness from the mass fraction is sensitive to the size of the nanoparticles. If compared on the basis of reduction capacity, the values obtained by XPS analysis and Cu(II) reduction experiments are in close agreement with a discrepancy of less than 7% (Table 2). The slightly lower reduction capacity obtained by the copper reduction experiments is to be expected because a small quantity of Fe^0 is inevitably consumed by reaction with water.

Overall the three methods yielded very similar results for the shell thickness, and this validates the determination and illustrates how these techniques can be used in a complementary approach for the study of the core−shell nanoparticles.

Table 2. Shell Thickness and Reductive Capacity of Iron Nanoparticles As Predicted by XPS Measurements and Cu(II) Reduction Experiments

	Cu(II) reduction experiments	XPS analysis
oxide shell thickness (nm)	∼3.4[a]	∼2.4
mass fraction of Fe^0 in nZVI (g of Fe^0/g of nanoparticles)	0.810	0.866[a]
Cu(II) reduction capacity (mequiv/g of nanoparticles)	29.0	31.0[a]

[a] Calculated on the basis of an average nanoparticle diameter of 60 nm.

In summary, we have presented a detailed characterization of the oxide/hydroxide shell thickness of nZVI nanoparticles using three independent methods. High-resolution TEM images provided direct evidence of the core−shell structure and indicated that fresh nZVI nanoparticles had a shell thickness of 2−4 nm. High-resolution XPS analysis, using the relative integrated intensities of metallic and oxidized iron with a geometric correction applied to account for the curved overlayer, yielded an average shell thickness in the range of 2.3−2.8 nm. The complete oxidation reaction of the nZVI particles by Cu(II) indicated a shell thickness (3.4 nm) consistent with these analyses. The three methods yielded very similar results, and thus, we have made a reliable determination of the shell thickness for fresh nZVI nanoparticles. This information fills an essential gap in our knowledge about the nZVI structure. In addition, we note that the methods presented in this work can also be applied to the study of the aging process of nZVI and may also prove useful for the measurement and characterization of other metallic nanoparticles.